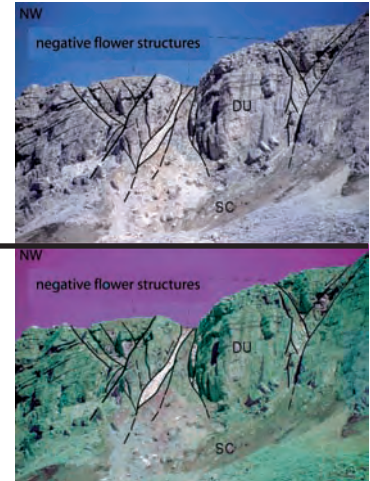


5. Strike-slip faults



Strike slip fault systems occur in all geodynamic settings, although they are typical of transform plate margins. Strike-slip systems are often segmented and show various fault arrangements (en-echelon, relay, anastomosing or stepping) (fig. 117). Strike slip faults are normally associated to other structures, such as synthetic and antithetic minor strike-slip faults, folds, normal and reverse faults (fig. 118). Oblique strike-slip motions (i.e., displacements characterised by a minor dip slip component) produce transpression (i.e., contractional deformation along the strike-slip fault) or transtension (i.e., dilational deformation along the fault).

In seismic sections strike slip fault zones are characterised by complex flower structures (figs. 119 - 123). Such structures are normally characterised by single or groups of steeply-dipping to vertical faults nucleating from the main strike-slip fault. These faults show either dominantly extensional (negative flower structures) or compressional (positive flower structures) displacements. Flower structures mainly develop at strike-slip fault bends that, depending on fault geometry and sense of shear, can be of two kinds: releasing bends,

associated to extension, and restraining bends, associated to shortening. Fault bends may also be associated to strike-slip extensional or contractional duplexes.

Strike-slip faults are often segmented and fault stepovers occur when single fault segments are arranged in en-echelon geometry. Stepovers of fault segments may drive to the development of contractional areas (restraining stepovers) and extensional areas (releasing stepovers). The most common structures associated to releasing stepovers are pull-apart basins (figs. 124 -128). At the tips of major strike-slip faults displacements die to zero. Slip is here accommodated by the formation of (both extensional or compressional) faults fans (fig. 129).

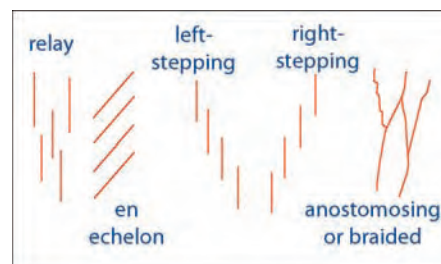


Fig. 117 - Typical geometry of strike-slip fault systems.

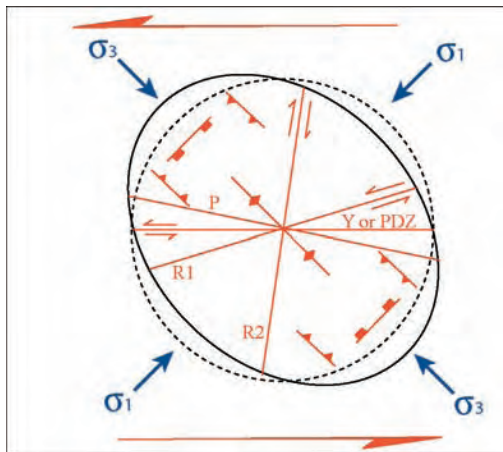


Fig. 118 - Structures associated to strike-slip faults. PDZ (principal displacement zone) or Y-Shear is the principal strike-slip zone. R1 (synthetic Riedel, at 15-20° to the PDZ) and R2 (antithetic Riedel at 70-75° to the PDZ) shears develop in response to Navier-Coulomb shear failure with respect to σ_1 and σ_3 . P synthetic shear develops at low angle (15°) to the PDZ as a consequence of the rotation of the principal stress axes at the tips of R1 shears as faulting develops. Minor thrust and normal faulting also may develop.

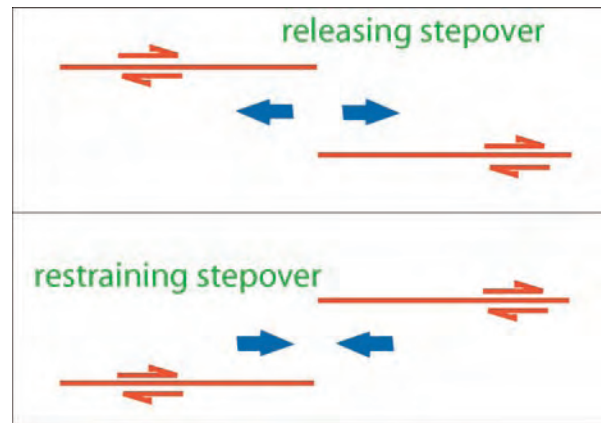


Fig. 120 - Strike slip segmentation and en-echelon stepover geometries may cause local shortening (restraining stepovers) or stretching (releasing stepovers). Stretching areas associated to releasing stepovers are called pull-apart basins, whereas the opposite restraining stepovers generate push-ups.

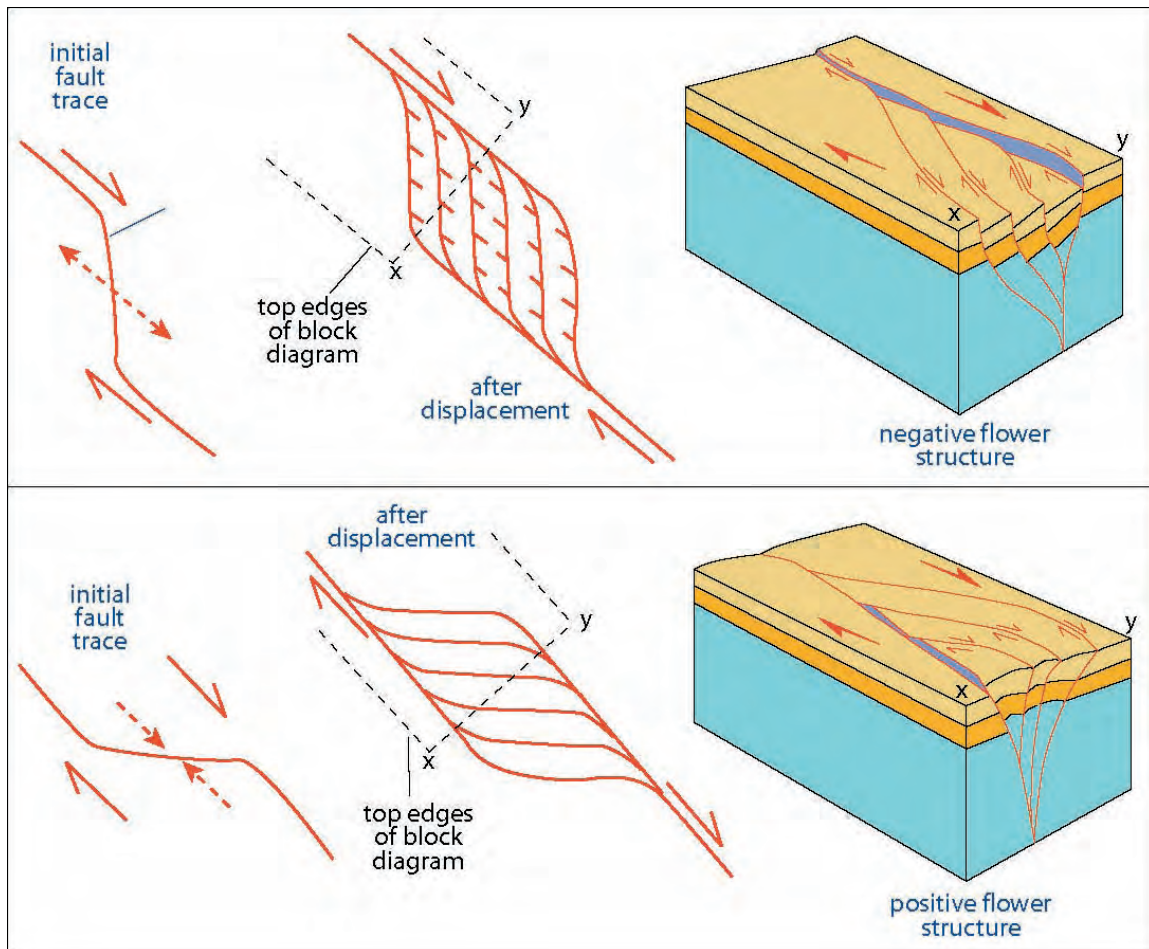


Fig. 119 - Undulated strike-slip faults give rise to local extensional (releasing bends; upper panel) or compressional (restraining bends; lower panel) zones. Releasing bends are associated to negative flower structures, whereas restraining bends to positive flower structures. In map view, these features are also called strike-slip duplexes. Modified after TWISS & MOORES (1992).

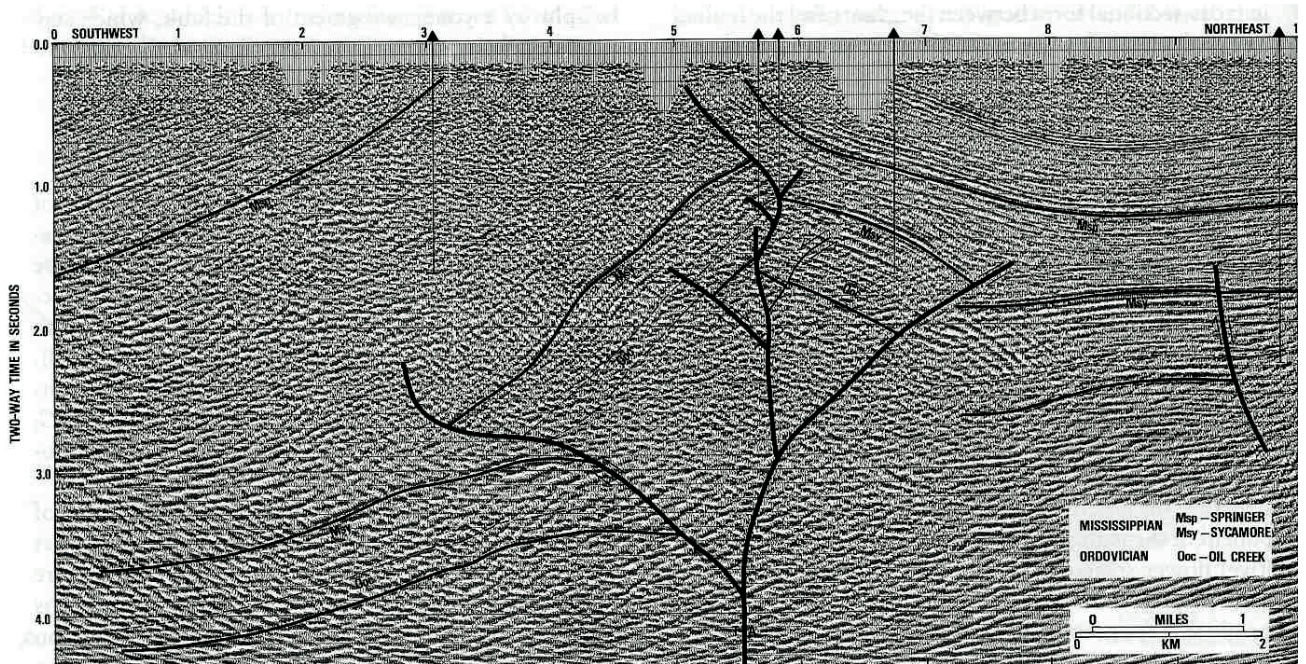
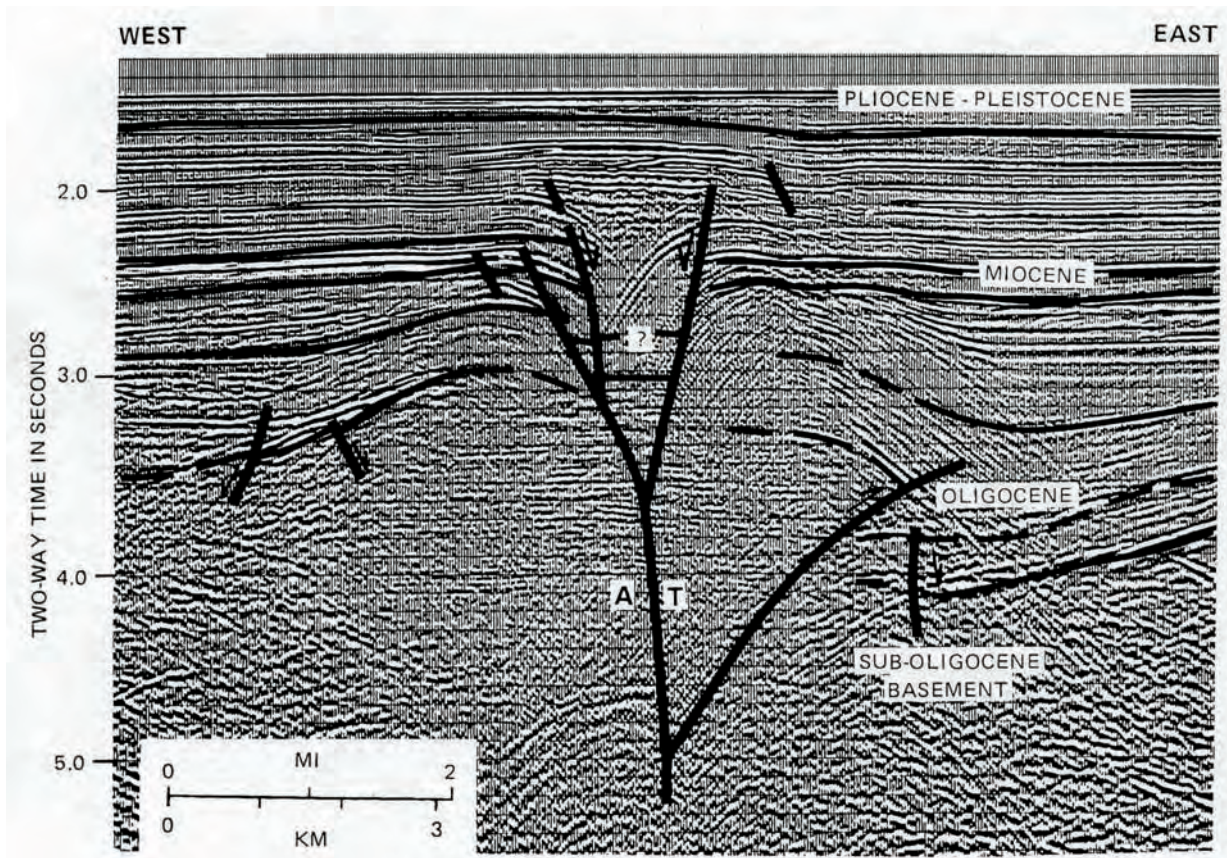


Fig. 121 - Seismic sections showing negative (above) and positive (below) flower structures. After HARDING (1983) and HARDING *et alii* (1983), in TWISS & MOORES (1992).

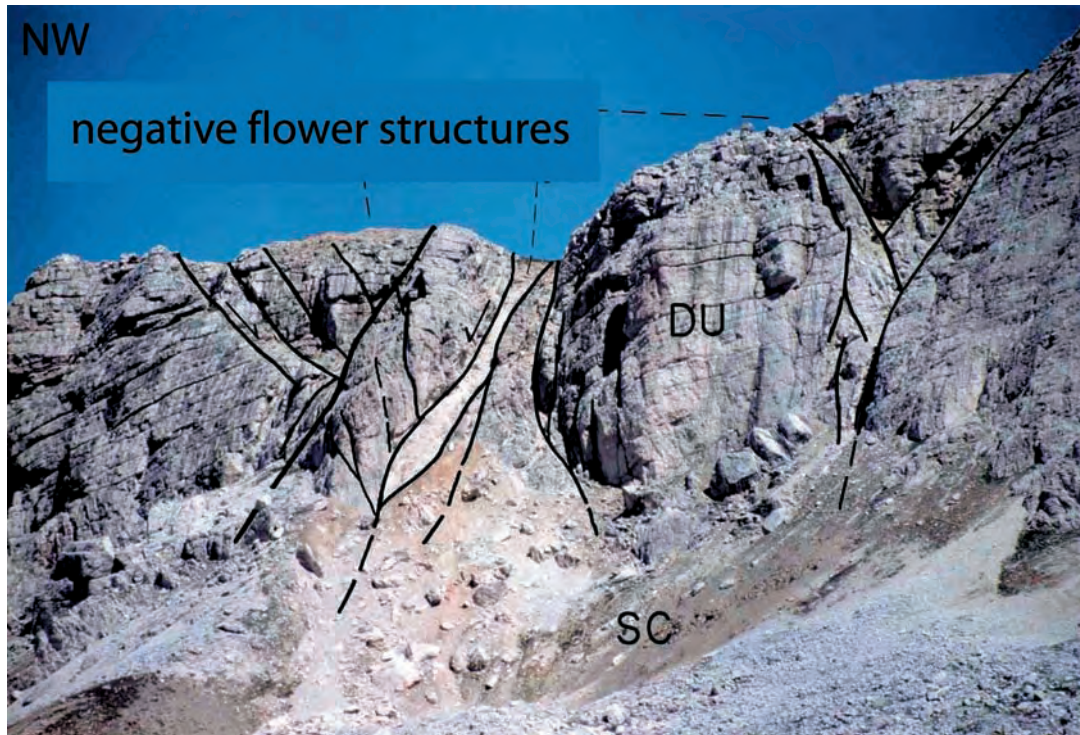


Fig. 122 - Negative flower structure related to sinistral strike-slip alpine tectonics in the SettSass Massif (Dolomites).

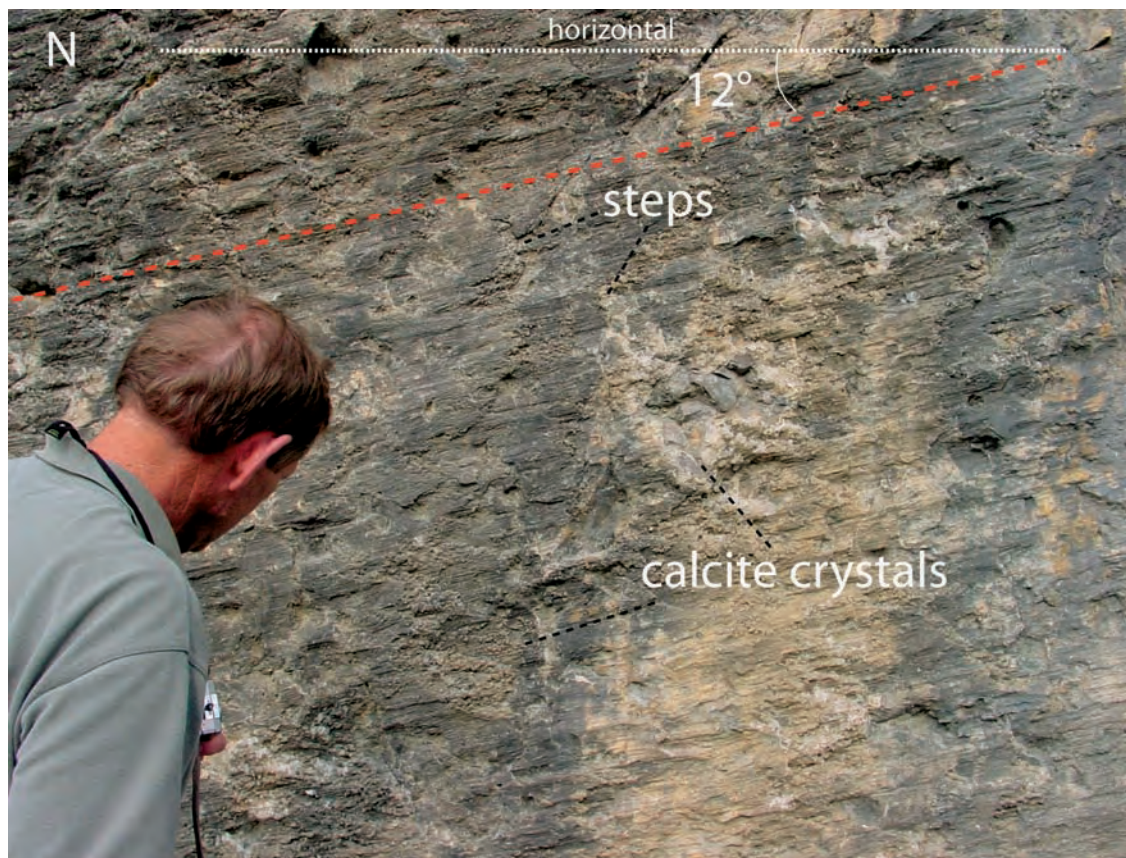


Fig. 123 - Transtensional N-S trending left-lateral fault in the Caotico Eterogeneo. Slickensides are more developed in conglomerates than in more homogeneous rocks. The striations have a pitch of 12° left (northward). The left-lateral sense of motion is indicated by the steps in the fault plane, and by the crystals of calcite grown in their shadow. Road between Caprile and Selva di Cadore (Dolomites). Casey Moore for scale.

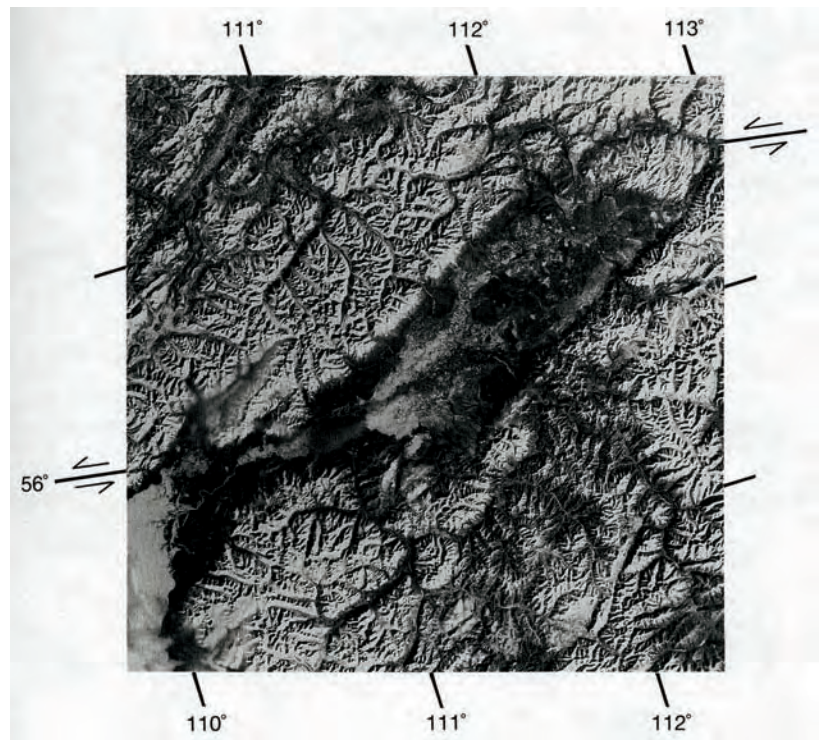


Fig. 124 - The Angara Graben is a pull apart basin northeast of Lake Baikal developed on a left steper in a left-lateral strike slip zone (after TAPPONNIER & MOLNAR, 1977).

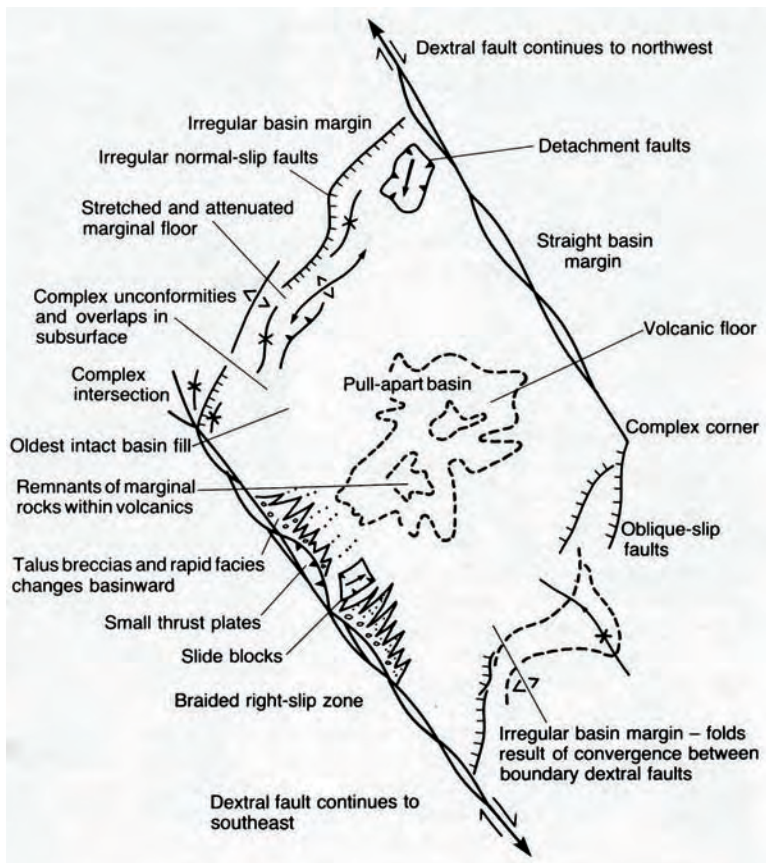


Fig. 125 - Tectonic structures and sedimentary features typical of pull apart basins. Subsidence may be abrupt and very fast. Volcanism may also be associated to extensional tectonics (after CROWELL, 1974).

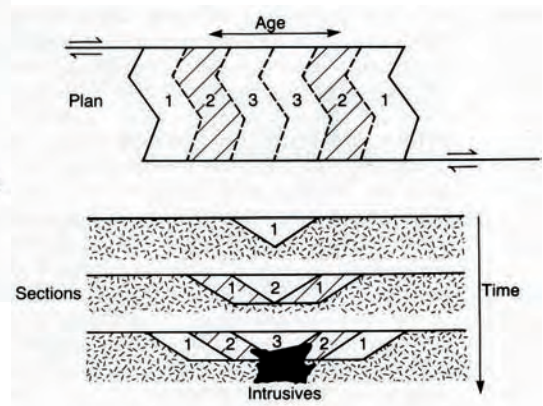


Fig. 126 - Stages of formation of a pull-apart basin (after KEAREY & VINE, 1992).

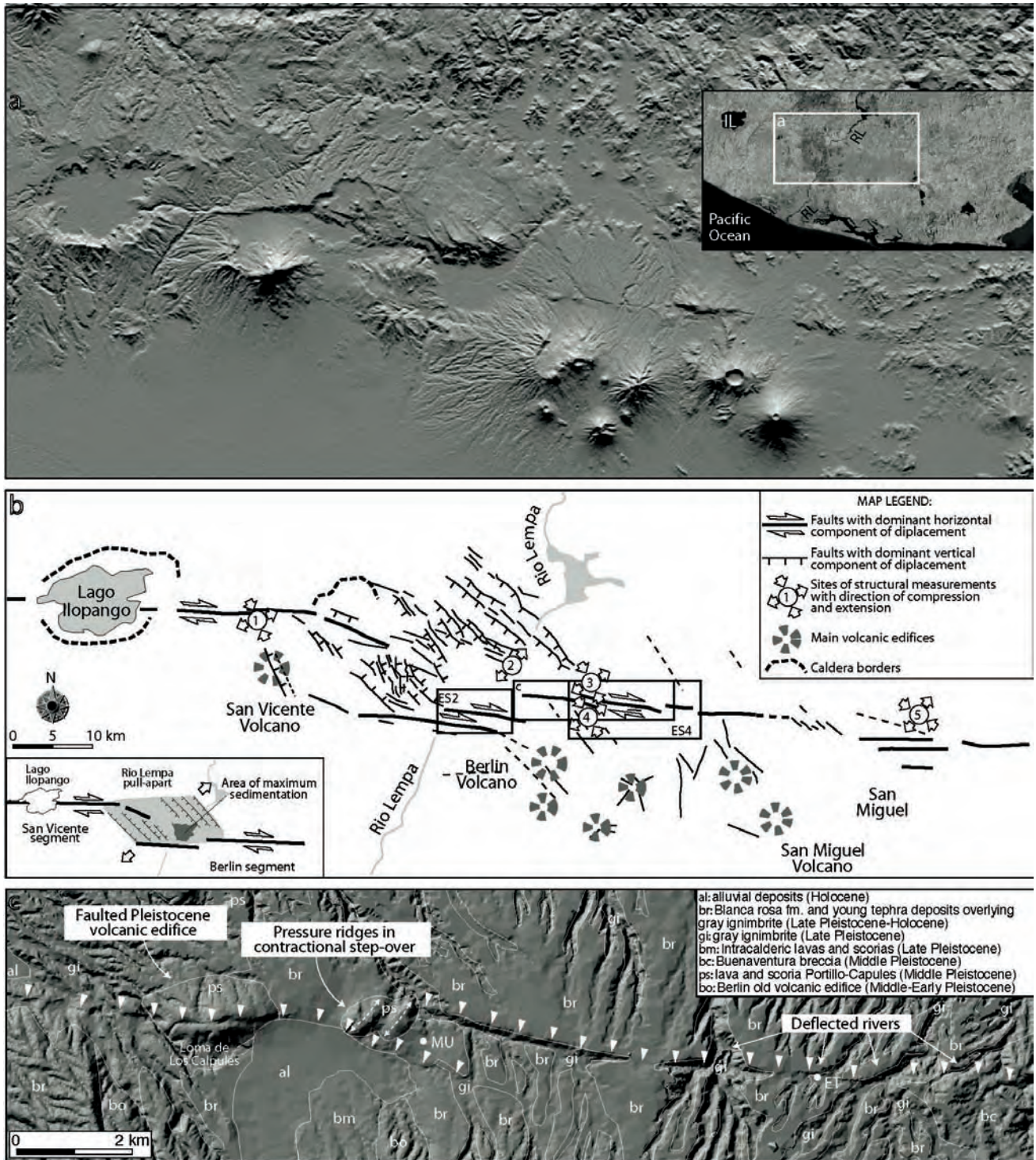


Fig. 127 - Along the El-Salvador fault zone, a major strike-slip fault system, the Rio Lempa pull-apart basin, developed in Quaternary times. (a) Digital elevation model of the region. (b) Line-drawing of the active structures forming the El Salvador Fault Zone (ESFZ) in the area, with also reported palaeostress orientations. Inset shows the interpretation of the regional fault pattern. (c) Geological map superimposed on a DEM of the region. Arrows indicate the fault trace. After CORTI *et alii* (2005).

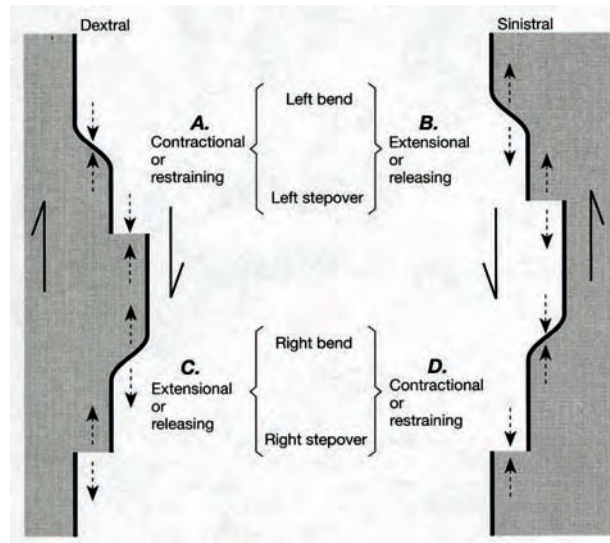


Fig. 128 - Terminology and stress state for bends and stepovers along strike-slip fault systems (after TWISS & MOORES, 1992).

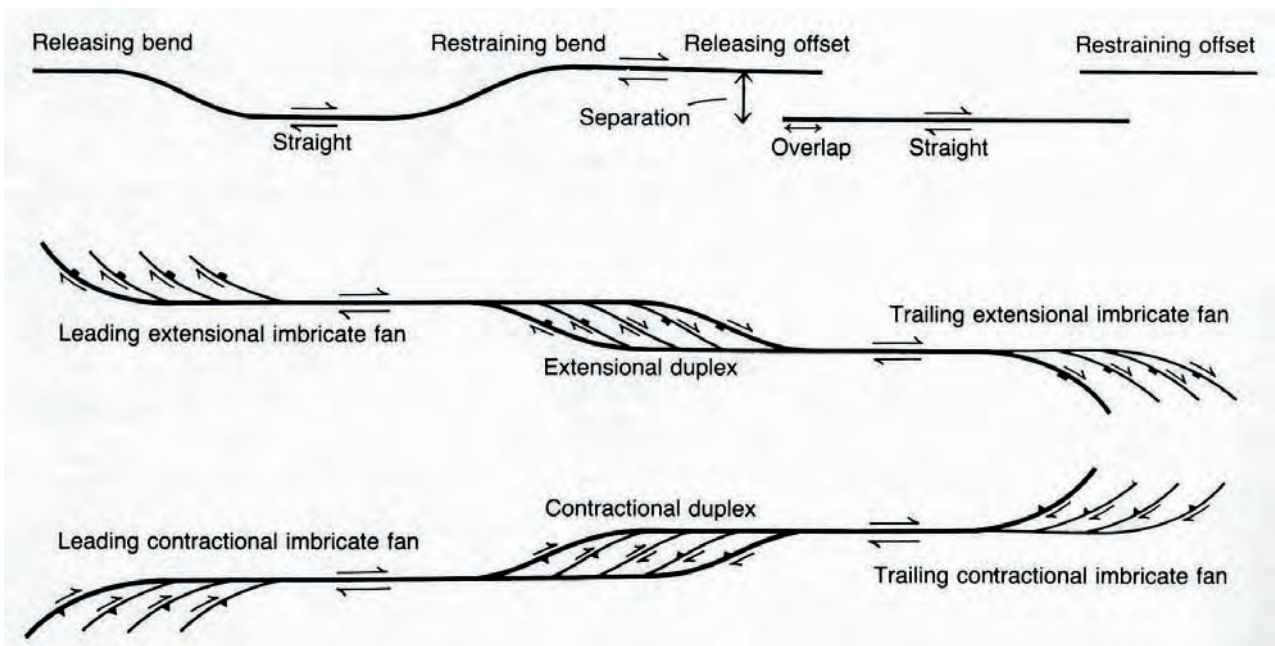
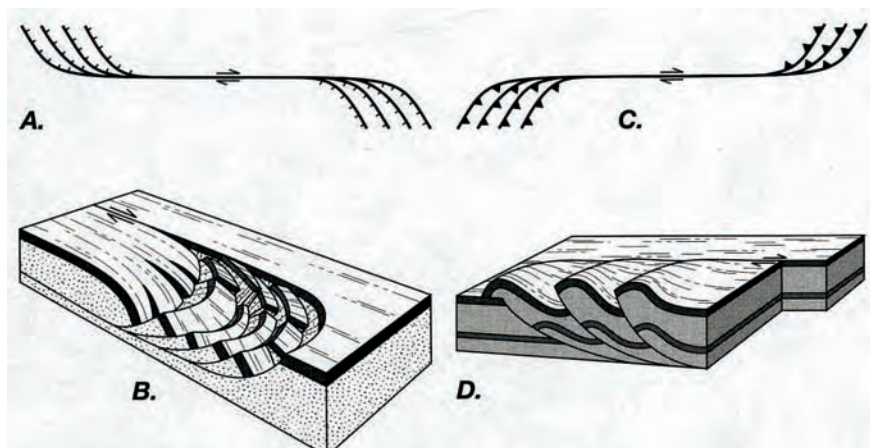
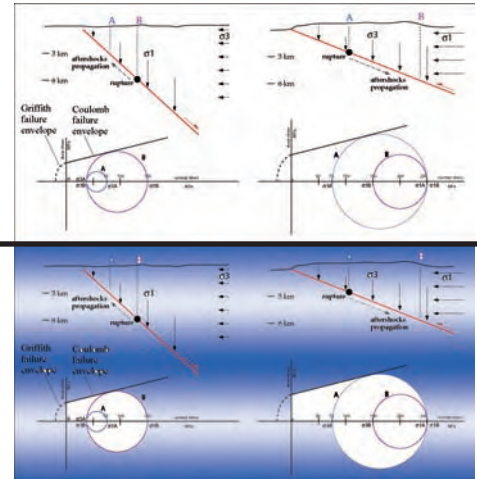


Fig. 129 - Strike-slip fault systems may include fault geometries similar to those of duplexes in contractional terrains. In this case however, the faults are subvertical and characterized mainly by strike-slip motion. Duplexes, either extensional or contractional, form at fault bends. At the termination of major strike slip faults, displacement may be accommodated by extensional (a,b) or contractional (c,d) imbricate fan structures. After WOODCOCK & FISHER (1986) and TWISS & MOORES (1992).



5.1 Opposite migration of seismicity



CARMINATI *et alii* (2004) showed that, along thrust faults, shallow initial rupture and downward migration of seismicity generally occur. On the contrary, along normal faults, rupture generally occurs at deeper levels and aftershocks are shallower. This opposite behavior is exemplified by Figs. 130 and 131 that show the opposite migration of seismicity associated to the Irpinia 1980 normal fault-related earthquake sequence and to the Friuli 1976 earthquake sequences occurred in a compressive environment.

This reverse behavior can be explained by a simple fault mechanical model.

The following discussion, based on Fig. 132, assumes that the pore fluid factor λ (equal to pore fluid pressure divided by the overburden pressure) is approximately constant with depth. It should be, however, noted that major differences from model predictions would occur with λ varying significantly with depth. Overpressured compartments bounded by sealing horizons (e.g., clay rich stratigraphic horizons or impermeable faults) are typical in sedimentary basins.

In crystalline rocks the base of the upper crustal hydrostatic fluid pressure regime is likely to be limited, during interseismic periods, to the first 3-7 km. This is in agreement with recent data from deep wells. Townsend and

Zoback (2000) analysed in situ stress and permeability measurements from deep (down to 9.1 km) boreholes and concluded that both these datasets suggest hydrostatic fluid pressures.

According to the Anderson fault theory, the vertical stress is the least principal stress in compressional regimes, whereas it is the maximum principal stress in extensional tectonic regimes.

Let us consider the state of stress of two points (A and B) positioned at different depths along hypothetical thrust and normal faults (Fig. 132).

Since A is shallower than B, the vertical load increases from point A to point B. It is here further assumed that the horizontal stress remains constant with depth. In compressional regimes the vertical load is σ_3 . Moving upward from location B to A, the differential stress (the diameter of the Mohr circle) increases.

As a consequence, moving upward along a thrust fault, the decrease of σ_3 enlarges the Mohr circle making the fault plane more unstable.

This means that rupture along the fault is likely to occur at shallower depths and that both the fracture and early aftershocks are expected to propagate downward, consistently with the

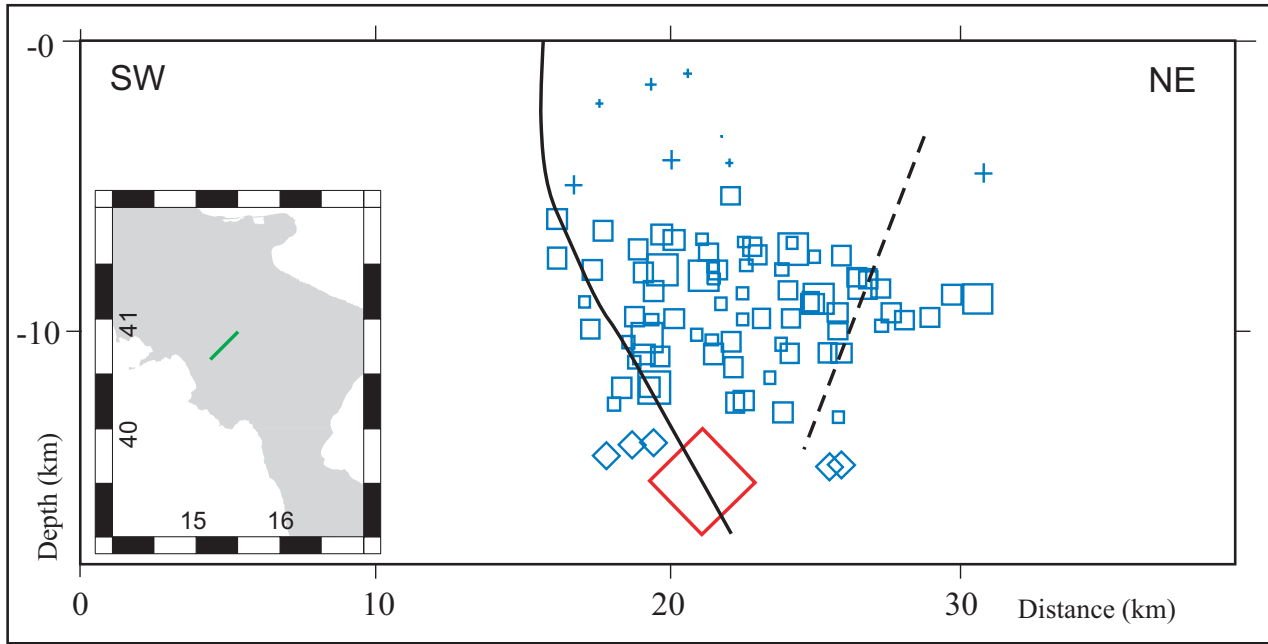


Fig. 130 - Cross-section of the Irpinia 1980 normal fault-related earthquake sequence. The largest red square is the mainshock. The blue squares are aftershocks. The earthquake was generated by two normal faults dipping north-eastward and one conjugate, and was characterised by Ms 6.9. The earthquake showed the largest moment release at a depth of 8-13 km and a possible nucleation at about 10 km. Most of the aftershocks were generated in the hanging wall of the main fault, between this and an antithetic normal fault dipping to the south-west. All the aftershocks occurred at depths (3-10 km) shallower than the mainshock. Modified after CARMINATI *et alii* (2004).

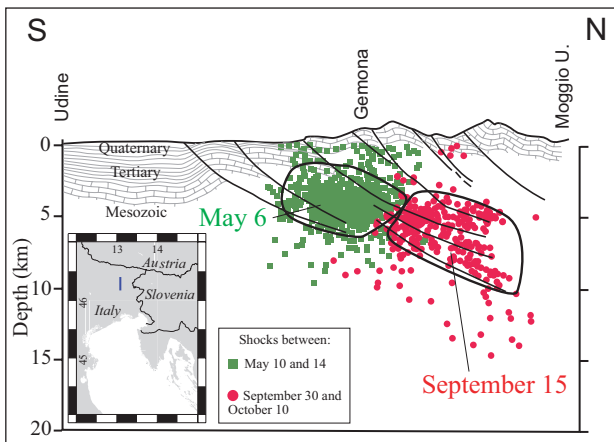


Fig. 131 - Cross-section of the Friuli 1976 earthquake sequences occurred in a compressive environment. The seismicity occurred in two main episodes, May 6 and September 15, with magnitude 6.4 and 6.1 respectively. The focal mechanisms are mainly compressional, with a slight transpressional component. They were associated with N-dipping thrust planes in the eastern part of the Southern Alps, at the intersection with the Dinarides thrust belt in north-east Italy. The maximum energy released by the aftershocks of the May 6 earthquake was very shallow, between 2 and 8 km. The highest energy release density has been evaluated to be located at a depth of about 4 km. The epicentres of the later September quakes and related aftershocks were about 8 km northward. The September hypocentres were deeper (down to 16-17 km) and characterised by a maximum energy release density at about 5-6 km. The timing of groups of events clearly shows a deepening of seismic activity with time. Modified after CARMINATI *et alii* (2004).

observations outlined above. On the other hand, if a small earthquake occurs at greater depths, it is unlikely to propagate upward and to grow into a larger one.

In extensional regimes the opposite occurs. The vertical load is σ_1 . Moving from location B to A the differential stress decreases. The decrease of σ_1 diminishes the Mohr circle making the fault plane more stable at shallower depth. As a consequence rupture is expected to occur, along normal faults, at deeper depths and early aftershocks are expected to propagate upwards, as observed in several natural cases.

Several researchers have proposed mechanical models assuming that non tectonic horizontal stress varies as $\sigma_h = [\nu / (1 - \nu)] \sigma_v$ (Poisson effect, see e.g., TWISS & MOORE, 1992), where ν is the Poisson's ratio (values between 0.25 and 0.33 are common for rocks). According to this relation, assuming $\nu = 0.25$, the non-tectonic component of horizontal stress is $\sigma_v / 3$.

This relation is based on the assumption that the uppermost brittle crust behaves elastically

and upper crustal rocks are laterally constrained (and therefore the horizontal strain is imposed equal to zero). Since we deal with the shallow brittle portion of the crust such

assumptions seem to be reasonable. Fig. 133 shows that, even considering a horizontal stress growing with depth, the above discussion holds.

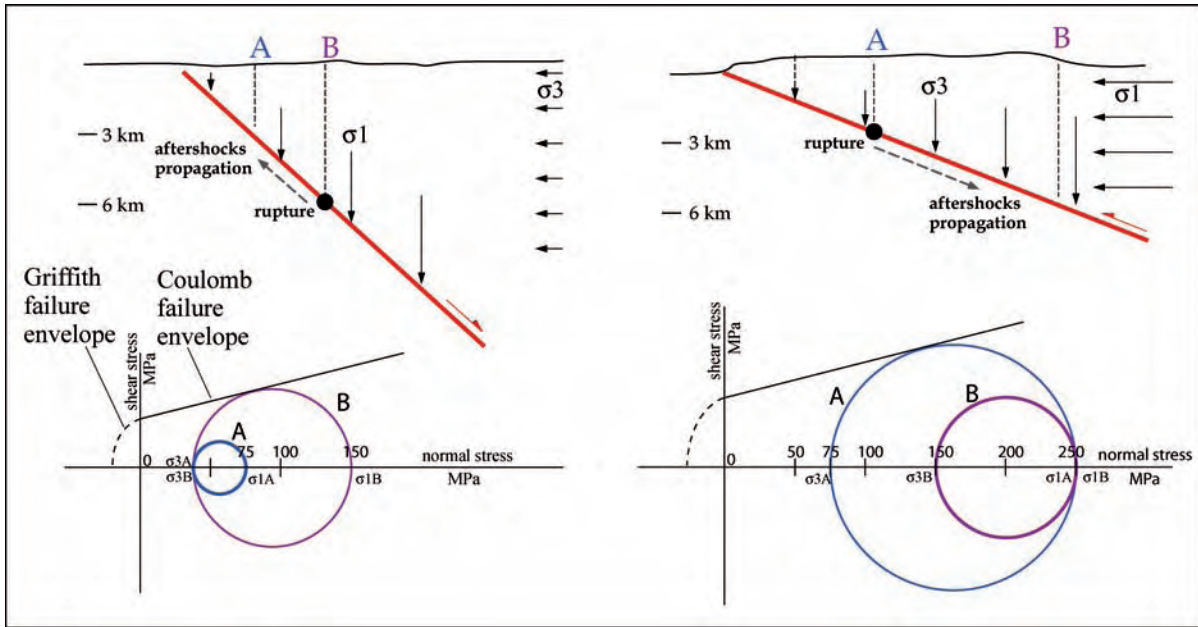


Fig. 132 - Left, sketch and Mohr diagram of the variation of σ_1 (vertical load) and σ_3 (horizontal load) along normal faults. Right, sketch and Mohr diagrams of the variation of σ_3 (vertical load) and σ_1 (horizontal load) along thrust faults. For the sake of simplicity horizontal stress is assumed to remain constant with depth. It is shown in the next figure that such a rough assumption does not hamper the validity of the model. Along thrust faults, shallow initial ruptures and downward migration of seismicity is more likely. On the contrary, along normal faults, rupture should generally occur at deeper levels and aftershocks are expected to be shallower.

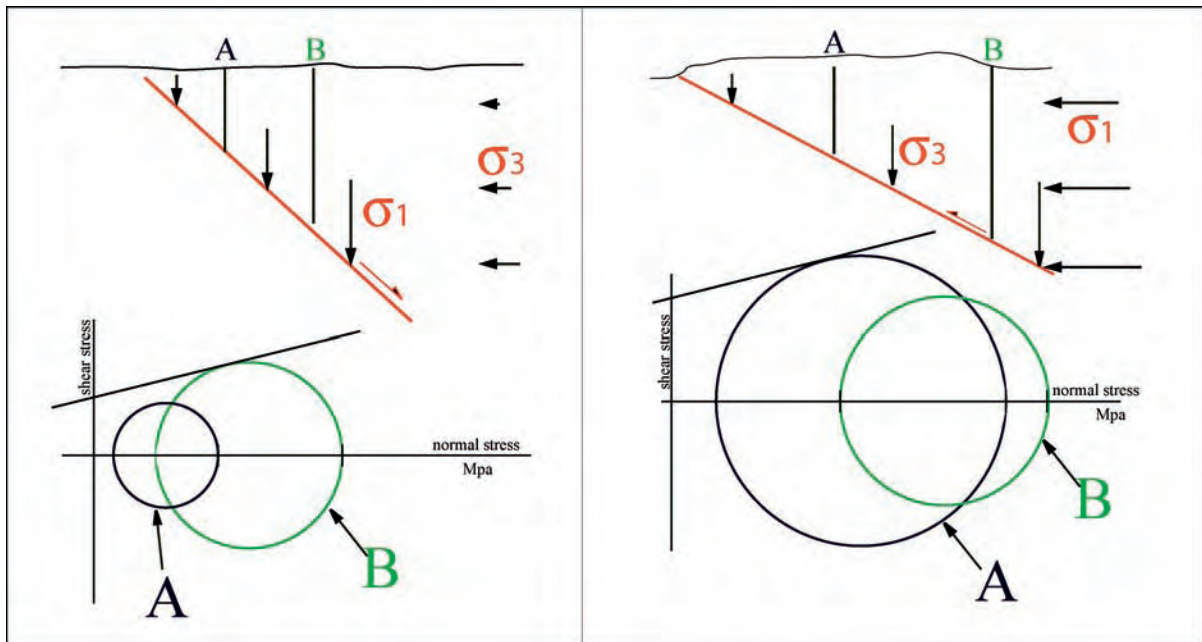


Fig. 133 - Left, sketch and Mohr diagram of the variation of σ_1 (vertical load) and σ_3 (horizontal load) along normal faults. Right, sketch and Mohr diagrams of the variation of σ_3 (vertical load) and σ_1 (horizontal load) along thrust faults. The horizontal stress increases with depth according to the Poisson effect. Along thrust faults, shallow initial ruptures and downward migration of seismicity is more likely. On the contrary, along normal faults, rupture should generally occur at deeper levels and aftershocks are expected to be shallower. Modified after CARMINATI *et alii* (2004).